

ESTIMATING THE AVERAGE SIZE OF FIBER/MATRIX INTERFACE CRACKS IN UD AND CROSS-PLY LAMINATES

L. Di Stasio^{1,2}, J. Varna¹, Z. Ayadi²

¹Division of Materials Science, Luleå University of Technology, Luleå, Sweden

²EEIGM & IJL, Université de Lorraine, Nancy, France

7th ECCOMAS Thematic Conference on the Mechanical Response of Composites
Girona (ES) - September 18-20, 2019



Education and Culture

Erasmus Mundus



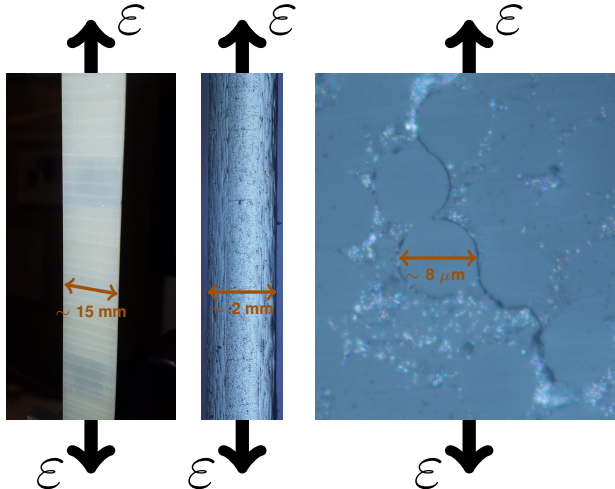
Outline

- Transverse Cracks Initiation in FRPC
- Modeling
- Debond Initiation
- Debond Propagation
- Conclusions



TRANSVERSE CRACKS INITIATION IN FRPC

Micromechanics of Initiation: Transverse Tensile Loading



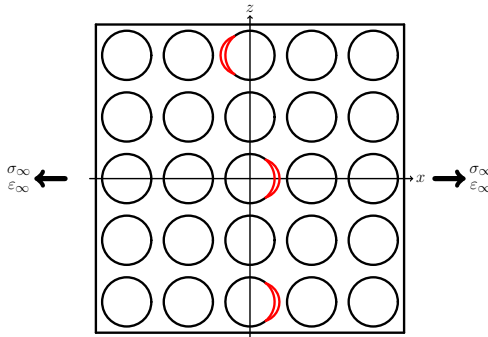
Left:
front view of $[0, 90_2]_S$,
visual inspection.

Center:
edge view of $[0, 90]_S$,
optical microscope.

Right:
edge view of $[0, 90]_S$,
optical microscope.

Micromechanics of Initiation: Transverse Tensile Loading

Stage 1: isolated debonds



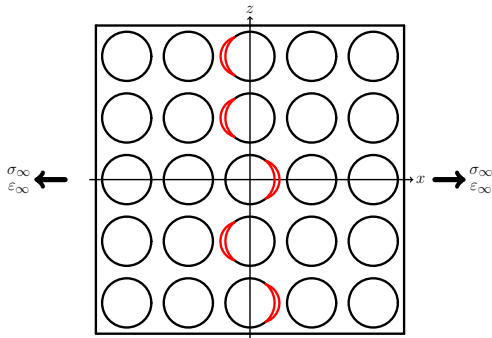
Bailey et al., P. Roy. Soc. A-Math. Phys. **366** (1727), 1979.

Bailey et al., J. Mater. Sci. **16** (3), 1981.

Zhang et al., Compos. Part A-Appl. S. **28** (4), 1997.

Micromechanics of Initiation: Transverse Tensile Loading

Stage 2: consecutive debonds



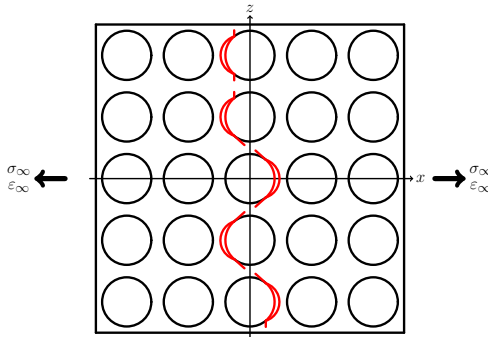
Bailey et al., P. Roy. Soc. A-Math. Phys. **366** (1727), 1979.

Bailey et al., J. Mater. Sci. **16** (3), 1981.

Zhang et al., Compos. Part A-Appl. S. **28** (4), 1997.

Micromechanics of Initiation: Transverse Tensile Loading

Stage 3: kinking



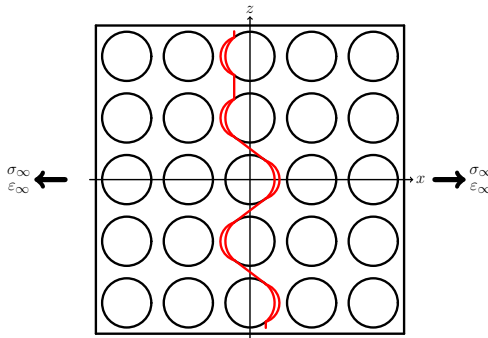
Bailey et al., P. Roy. Soc. A-Math. Phys. **366** (1727), 1979.

Bailey et al., J. Mater. Sci. **16** (3), 1981.

Zhang et al., Compos. Part A-Appl. S. **28** (4), 1997.

Micromechanics of Initiation: Transverse Tensile Loading

Stage 4: coalescence



Bailey et al., P. Roy. Soc. A-Math. Phys. **366** (1727), 1979.

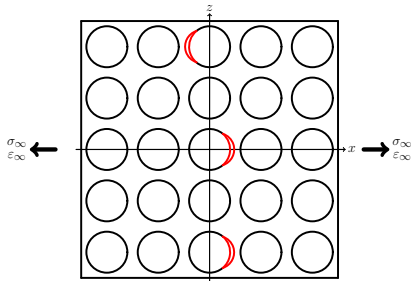
Bailey et al., J. Mater. Sci. **16** (3), 1981.

Zhang et al., Compos. Part A-Appl. S. **28** (4), 1997.

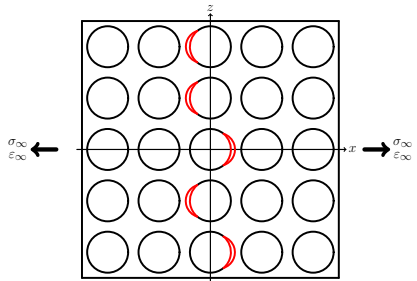
Objective of the Study

Can we talk about a ply-thickness effect for the fiber-matrix interface crack?

Stage 1: isolated debonds

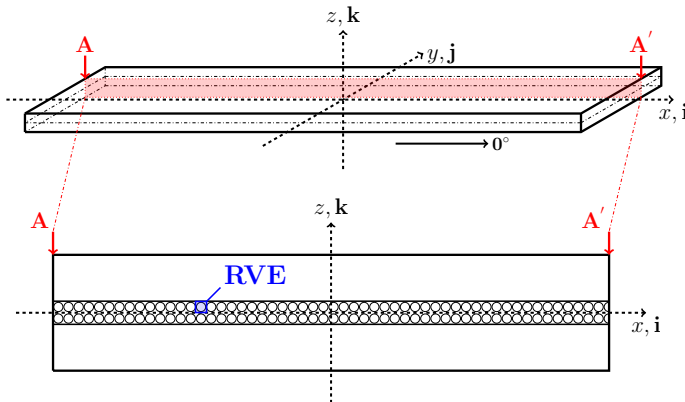


Stage 2: consecutive debonds



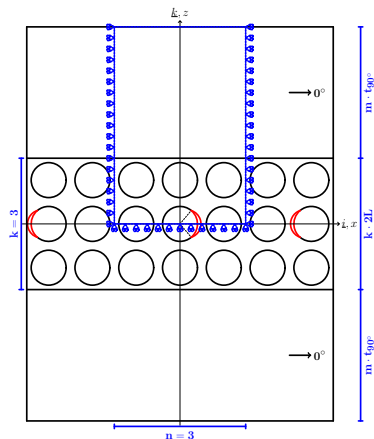
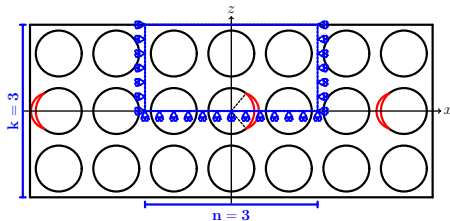
MODELING

Geometry

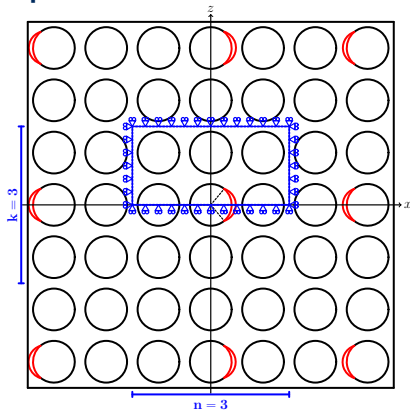


- $L, W \gg t$
- $L, W \rightarrow \infty$
- Square packing
- $L_d \gg \Delta\theta_d$
- 2D RVE

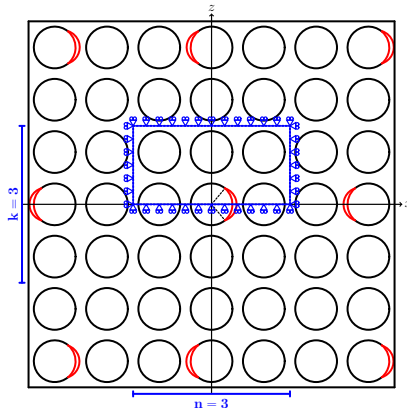
Representative Volume Elements



Representative Volume Elements

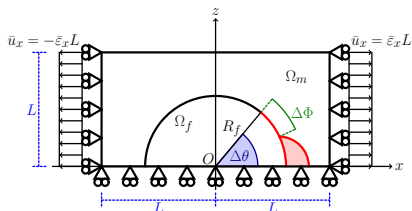


$n \times k - \text{symm}$



$n \times k - \text{asymm}$

Assumptions

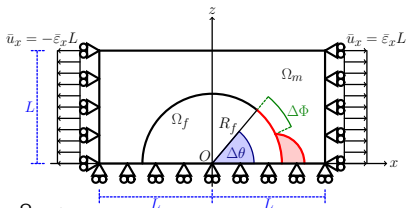


$$R_f = 1 \text{ } [\mu\text{m}] \quad L = \frac{R_f}{2} \sqrt{\frac{\pi}{V_f}}$$

- Linear elastic, homogeneous materials
- Concentric Cylinders Assembly with Self-Consistent Shear Model for UD
- Plane strain
- Frictionless contact interaction
- Symmetric w.r.t. x-axis
- Coupling of x-displacements on left and right side (repeating unit cell)
- Applied uniaxial tensile strain $\bar{\epsilon}_x = 1\%$
- $V_f = 60\%$

Material	V_f [%]	E_L [GPa]	E_T [GPa]	μ_{LT} [GPa]	ν_{LT} [-]	ν_{TT} [-]
Glass fiber	-	70.0	70.0	29.2	0.2	0.2
Epoxy	-	3.5	3.5	1.25	0.4	0.4
UD	60.0	43.442	13.714	4.315	0.273	0.465

Solution



in $\Omega_f, \Omega_m, \Omega_{UD}$:

$$\frac{\partial^2 \varepsilon_{xx}}{\partial z^2} + \frac{\partial^2 \varepsilon_{zz}}{\partial x^2} = \frac{\partial^2 \gamma_{zx}}{\partial x \partial z} \quad \text{for } 0^\circ \leq \alpha \leq \Delta\theta, \Delta\theta \neq 0^\circ :$$

$$(\vec{u}_m(R_f, \alpha) - \vec{u}_f(R_f, \alpha)) \cdot \vec{n}_\alpha \geq 0$$

$$\varepsilon_y = \gamma_{xy} = \gamma_{yz} = 0$$

$$\frac{\partial \sigma_{xx}}{\partial x} + \frac{\partial \tau_{zx}}{\partial z} = 0$$

$$\frac{\partial \tau_{zx}}{\partial x} + \frac{\partial \sigma_{zz}}{\partial z} = 0$$

$$\sigma_{yy} = \nu (\sigma_{xx} + \sigma_{zz})$$

for $\Delta\theta \leq \alpha \leq 180^\circ$:

$$\vec{u}_m(R_f, \alpha) - \vec{u}_f(R_f, \alpha) = 0$$

$$\sigma_{ij} = E_{ijkl} \varepsilon_{kl} + BC$$

$$\forall \Delta\theta \neq 0^\circ$$

→ oscillating singularity

$$\sigma \sim r^{-\frac{1}{2}} \sin(\varepsilon \log r), \quad V_f \rightarrow 0$$

$$\varepsilon = \frac{1}{2\pi} \log \left(\frac{1 - \beta}{1 + \beta} \right)$$

$$\beta = \frac{\mu_2 (\kappa_1 - 1) - \mu_1 (\kappa_2 - 1)}{\mu_2 (\kappa_1 + 1) + \mu_1 (\kappa_2 + 1)}$$

→ receding contact

$$\rightarrow \frac{G(R_{f,2})}{G(R_{f,1})} = \frac{R_{f,2}}{R_{f,1}}, \quad \frac{G(\bar{\varepsilon}_{x,2})}{G(\bar{\varepsilon}_{x,1})} = \frac{\bar{\varepsilon}_{x,2}^2}{\bar{\varepsilon}_{x,1}^2}$$

→ FEM + LEFM (VCCT)

→ regular mesh of quadrilaterals at the crack tip:

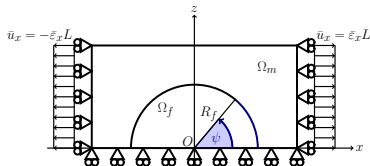
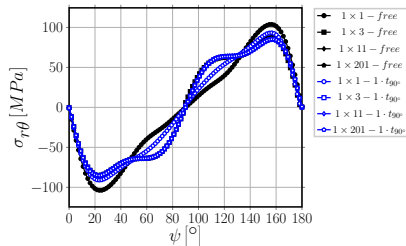
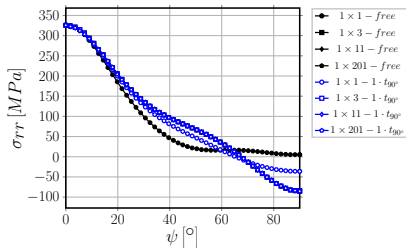
$$- AR \sim 1, \quad \delta = 0.05^\circ$$

$$\forall \Delta\theta$$

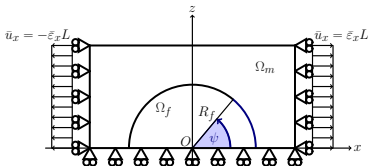
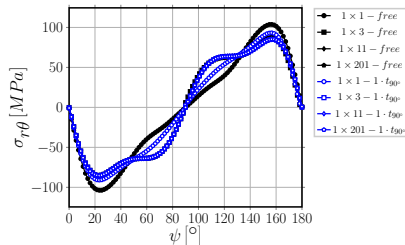
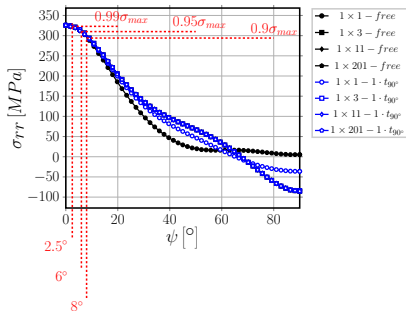
→ 2nd order shape functions

➤ DEBOND INITIATION

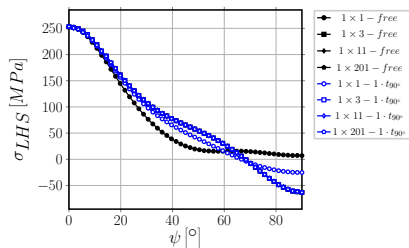
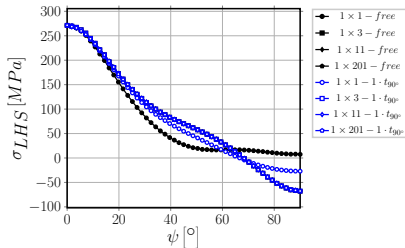
σ_{rr} VS $\tau_{r\theta}$: radial stress vs tangential shear at the interface



σ_{rr} VS $\tau_{r\theta}$: radial stress vs tangential shear at the interface

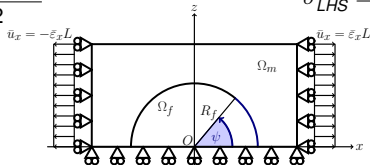


σ_{LHS} : local hydrostatic stress at the interface

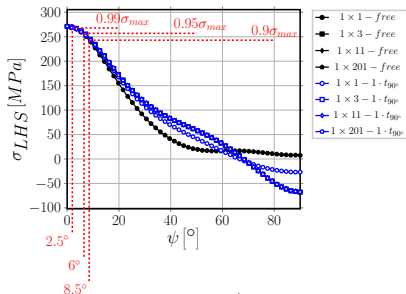


$$\sigma_{LHS}^{2D} = \frac{\sigma_{rr} + \sigma_{\theta\theta}}{2}$$

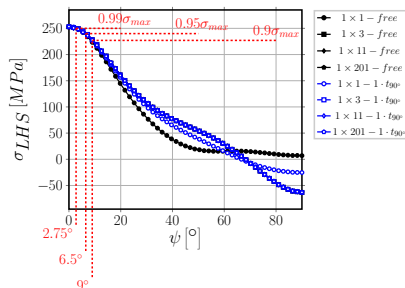
$$\sigma_{LHS}^{3D} = \frac{\sigma_{rr} + \sigma_{\theta\theta} + \sigma_{yy}}{3}$$



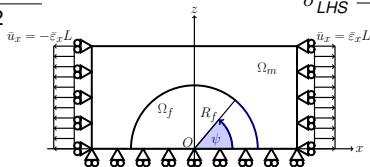
σ_{LHS} : local hydrostatic stress at the interface



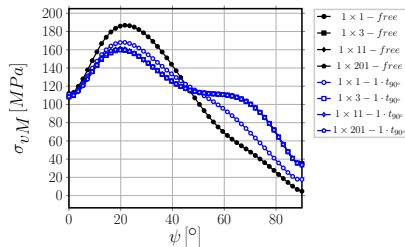
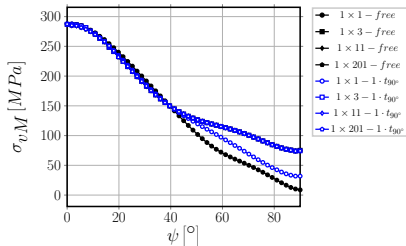
$$\sigma_{LHS}^{2D} = \frac{\sigma_{rr} + \sigma_{\theta\theta}}{2}$$



$$\sigma_{LHS}^{3D} = \frac{\sigma_{rr} + \sigma_{\theta\theta} + \sigma_{yy}}{3}$$

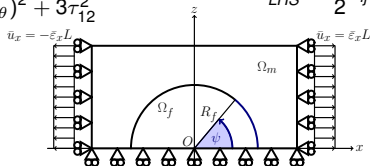


σ_{vM} : von Mises stress at the interface

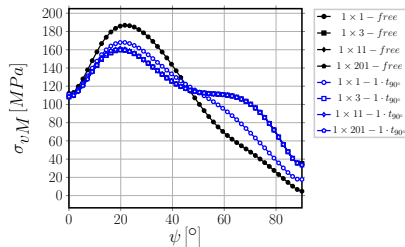
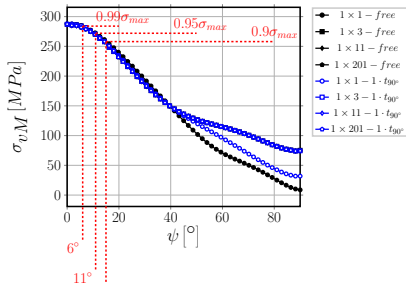


$$\sigma_{vM}^{2D} = \sqrt{(\sigma_{rr} - \sigma_{\theta\theta})^2 + 3\tau_{12}^2}$$

$$\sigma_{LHS}^{3D} = \frac{3}{2} s_{ij} s_{ij} \quad s_{ij} = \sigma_{ij} - \frac{1}{3} \sigma_{kk} \delta_{ij}$$

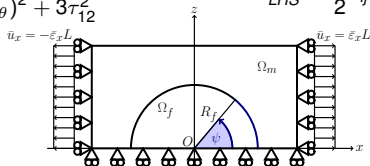


σ_{vM} : von Mises stress at the interface

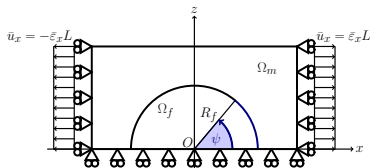
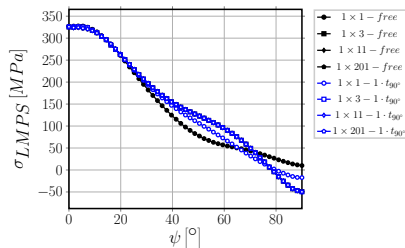
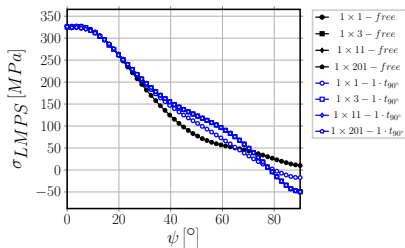


$$\sigma_{vM}^{2D} = \sqrt{(\sigma_{rr} - \sigma_{\theta\theta})^2 + 3\tau_{12}^2}$$

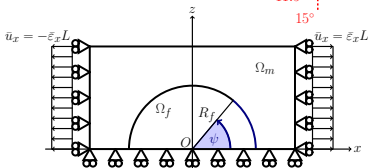
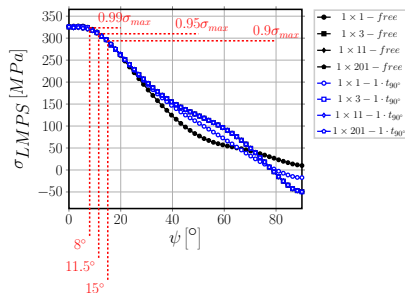
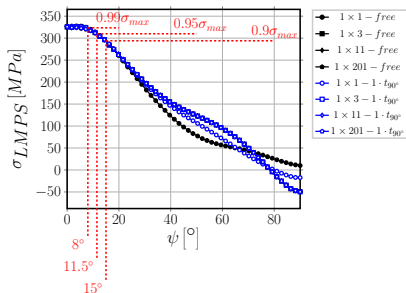
$$\sigma_{LHS}^{3D} = \frac{3}{2} s_{ij} s_{ij} \quad s_{ij} = \sigma_{ij} - \frac{1}{3} \sigma_{kk} \delta_{ij}$$



σ_I : maximum principal stress at the interface



σ_I : maximum principal stress at the interface

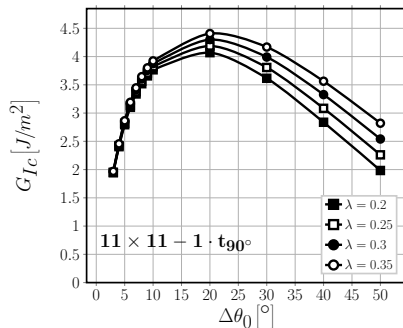
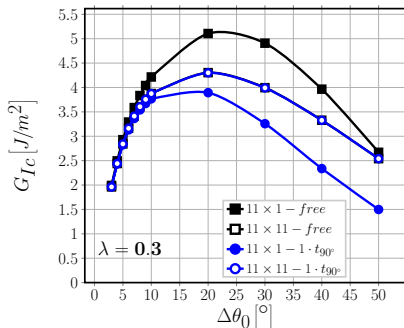


Summary



DEBOND PROPAGATION

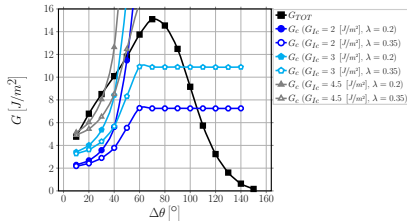
Estimation of G_{Ic}



$$G_{Ic} = \frac{G_c}{1 + \tan^2((1 - \lambda) \Psi_G)} \Big|_{G_c = G_{TOT}(\Delta\theta_0)}, \quad \Psi_G = \tan^{-1} \left(\sqrt{\frac{G_{II}}{G_I}} \right) \Big|_{\Delta\theta_0}$$

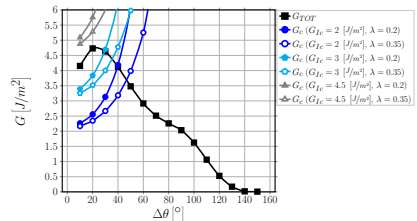
Estimation of $\Delta\theta_{max}$

$21 \times 1 - free$



$$\Delta\theta_{max} \in (30^\circ - 105^\circ)$$

$21 \times 1 - 1 \cdot t_{90^\circ}$

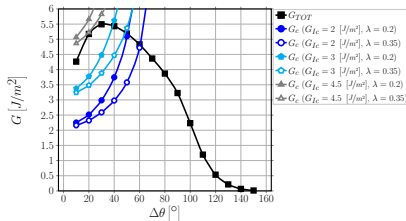


$$\Delta\theta_{max} \in (30^\circ - 50^\circ)$$

$$G_{TOT}(\Delta\theta) > G_c = G_{Ic} \left(1 + \tan^2((1 - \lambda) \Psi_G) \right), \quad \Psi_G = \tan^{-1} \left(\sqrt{\frac{G_{II}}{G_I}} \right) \Big|_{\Delta\theta}$$

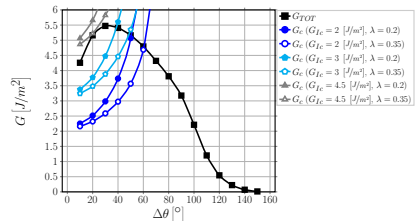
Estimation of $\Delta\theta_{max}$

$21 \times 3 - free$



$\Delta\theta_{max} \in (40^\circ - 60^\circ)$

$21 \times 3 - 1 \cdot t_{90^\circ}$

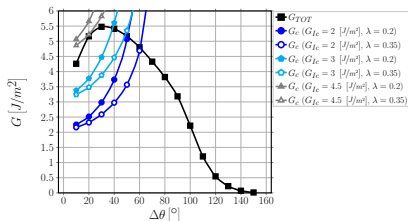


$\Delta\theta_{max} \in (40^\circ - 60^\circ)$

$$G_{TOT}(\Delta\theta) > G_c = G_{Ic} \left(1 + \tan^2((1 - \lambda) \Psi_G) \right), \quad \Psi_G = \tan^{-1} \left(\sqrt{\frac{G_{II}}{G_I}} \right) \Big|_{\Delta\theta}$$

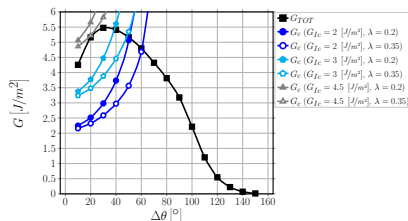
Estimation of $\Delta\theta_{max}$

$21 \times 21 - free$



$$\Delta\theta_{max} \in (40^\circ - 60^\circ)$$

$21 \times 21 - 1 \cdot t_{90^\circ}$

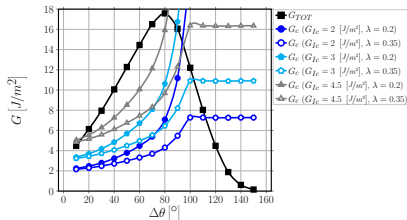


$$\Delta\theta_{max} \in (40^\circ - 60^\circ)$$

$$G_{TOT}(\Delta\theta) > G_c = G_{Ic} \left(1 + \tan^2((1 - \lambda) \Psi_G) \right), \quad \Psi_G = \tan^{-1} \left(\sqrt{\frac{G_{II}}{G_I}} \right) \Big|_{\Delta\theta}$$

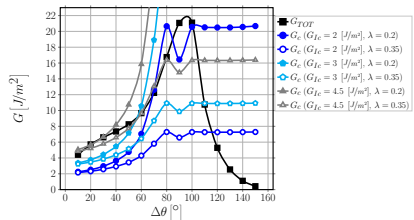
Estimation of $\Delta\theta_{max}$

21 × 21 – *symm*



$\Delta\theta_{max} \in (80^\circ - 110^\circ)$

21 × 21 – *asymm*



$\Delta\theta_{max} \in (55^\circ - 115^\circ)$

$$G_{TOT}(\Delta\theta) > G_c = G_{Ic} \left(1 + \tan^2((1 - \lambda) \Psi_G) \right), \quad \Psi_G = \tan^{-1} \left(\sqrt{\frac{G_{II}}{G_I}} \right) \Big|_{\Delta\theta}$$

CONCLUSIONS

Conclusions

- No effect of 90° ply thickness can be observed when t_{90° is at least $\sim 3 \varnothing_{fiber}$
- Only if t_{90° is reduced to $1 \varnothing_{fiber}$, ERR is reduced for a given level of applied strain, i.e. debond growth is delayed to higher levels of applied strain ($G \sim \varepsilon_{applied}^2$)
- No effect of 0° ply thickness can be observed when $t_{0^\circ}/t_{90^\circ} > 1$
- A small difference can be observed when $t_{0^\circ} = t_{90^\circ}$, due to the smaller bending stiffness of a thinner 0° layer

